The Astrophysical Journal, 459:L35–L38, 1996 March 1

GIANT PLANETS AT SMALL ORBITAL DISTANCES

T. Guillot,[1] A. Burrows,[2] W. B. Hubbard,[1] J. I. Lunine,[1] and D. Saumon[1,3]
Received 1995 November 8; accepted 1995 December 19

ABSTRACT

Using Doppler spectroscopy to detect the reflex motion of the nearby star, 51 Pegasi, Mayor & Queloz (1995) claim to have discovered a giant planet in a 0.05 AU, 4.23 day orbit. They estimate its mass to be in the range 0.5–2 Jupiter masses, but are not able to determine its nature or origin. Including the effects of the severe stellar insolation implied, we extend the theory of giant planets we have recently developed to encompass those at very small orbital distances. Our calculations can be used to help formulate search strategies for luminous planets in tight orbits around other nearby stars. We calculate the radii and luminosities of such giant planets for a variety of compositions (H/He, He, H_2O, and olivine), the evolutionary tracks for solar-composition gas giants, and the geometry of the Hayashi forbidden zone in the gas-giant mass regime. We show that such planets are stable and estimate the magnitude of classical Jeans evaporation and of photodissociation and loss due to EUV radiation. In addition, we demonstrate that for the mass range quoted, such planets are well within their Roche lobes. We show that the strong composition dependence of the model radii and the distinctive spectral signatures provide clear diagnostics that might reveal 51 Peg B's nature, should interferometric or adaptive-optics techniques ever succeed in photometrically separating planet from star.

Subject headings: stars: individual (51 Pegasi) — planetary systems — planets and satellites: general

1. INTRODUCTION

As the search for planets and brown dwarfs around nearby stars accelerates, we should expect to be surprised. In no instance is this better illustrated than in the recent discovery by Mayor & Queloz (1995) of a planet orbiting a G2.5 star, 51 Pegasi, 14 parsecs away. With a 4.23 day period, a semimajor axis of 0.05 AU, an eccentricity less than 0.15, and an inferred mass between 0.5 and 2 Jupiter masses (M_J), this object is certainly problematic. As of this writing, the telltale periodic Doppler shift in the spectral lines of the primary had been confirmed by Marcy & Butler (1995) and by Noyes et al. (1995). A good case can be made for the existence of 51 Peg B simply from the absence of significant photometric variations in V (<0.002 mag; Mayor & Queloz 1995; Burki, Burnet, & Kuenzli 1995) or asymmetries in the line profiles (Mayor & Queloz 1995), and from the difficulty of explaining such a period as pulsation of a near-solar analog.

One hundred times closer to its primary than Jupiter itself, 51 Peg B thwarts conventional wisdom. Boss (1995) had argued that the nucleation of a H/He-rich Jovian planet around a rock and ice core could be achieved in a protostellar disk only at and beyond the ice point (at ∼160 K) exterior to 4 AU. Walker et al. (1995) had surveyed 21 G-type stars for reflex motion over 12 years, had detected none, and had derived upper limits of 0.5–3 M_J for the masses (modulo sin i) of the interior of any planet, to ∼6 AU, that they may have missed. Zuckermann, Forveille, & Kastner (1995) had measured CO emissions from a variety of near–T Tauri disks, had extrapolated to H_2, and had concluded that there may not be enough mass or time to form a Jupiter around a majority of stars. The discovery of 51 Peg B, while not strictly inconsistent with any of these papers, vastly enlarges the parameter space within which we must now search.

Several scenarios for the origin of 51 Peg B are emerging.

1. It could be a canonical gas giant that formed many AUs from 51 Peg A, but through frictional and tidal effects spiraled inward during the protostellar phase (Lin, Bodenheimer, & Richardson 1995).
2. It could be composed predominantly of hydrogen and helium accreted from the protostellar disk, but nucleated in situ around a large rock core (without ice).
3. It could be a giant terrestrial planet formed by the accumulation of planetesimals.
4. It could be an evaporated, ablated, or tidally stripped brown dwarf or star.

However, whatever the provenance or evolutionary history of 51 Peg B, a knowledge of the thermal and structural characteristics of giant planets with a variety of compositions and masses (M_p) is required to understand it and others like it. A chondritic, helium, or ice planet with a mass of ∼1 M_J has a radius (R_p) that is significantly smaller than that of a hydrogen-rich Jupiter. At a given effective temperature ($T_{\rm eff}$), smaller radii translate into smaller luminosities (L).

Recently, we have studied the theoretical evolution of gas giants with masses from 0.3 through 15 M_J and of brown dwarfs/M dwarfs with masses from 10 through 250 M_J (Saumon et al. 1996; Burrows et al. 1995; Saumon et al. 1994; Burrows et al. 1993; Burrows, Hubbard, & Lunine 1989). Though we had previously considered the effects of stellar insolation, we had not explored such effects at separations near those of 51 Peg B. In this Letter, we present a theory of extrasolar giant planets at small orbital distances (D). We calculate the radii and luminosities of planets with a variety of compositions, masses, and separations. Though we focus on the 51 Peg system, our results can be extended and scaled to planetary systems with other characteristics and are meant to aid in the formulation of search strategies around nearby stars. In addition, we explore the possibilities of tidal truncation and

[1] Department of Planetary Sciences, University of Arizona, Tucson, AZ 85721; guillot, hubbard, jlunine, dsaumon@lpl.arizona.edu.
[2] Departments of Physics and Astronomy, University of Arizona, Tucson, AZ 85721; burrows@cobalt.physics.arizona.edu.
[3] Hubble Postdoctoral Fellow.

evaporation, and conclude with a discussion on the photometric and spectroscopic discriminants of the various theories concerning the nature of 51 Peg B.

2. THE RADII OF GIANT PLANETS AS A FUNCTION OF COMPOSITION

The method used for this study is described by Saumon et al. (1996). The hydrogen/helium equation of state is that of Saumon, Chabrier, & Van Horn (1995), which incorporates state-of-the-art prescriptions for the interactions among H_2, H, protons, and electrons and for the metallization of hydrogen/helium mixtures at high pressures. Model atmospheres, including the possible presence of clouds, were taken from Burrows et al. (1993). However, the case of 51 Peg B is different from those studied by Saumon et al. (1996). Proximity to a central star produces significant external heating and the planet soon develops an outer radiative zone (it is no longer fully convective). Therefore, we used the code of Guillot & Morel (1995), which treats the evolution problem as an implicit two-point boundary problem. This code was originally constructed to address the possibility that Jupiter and Saturn may have nonadiabatic structures (Guillot et al. 1995). We used opacities calculated by Alexander & Ferguson (1994), and both the internal flux and external heating by the star were included.

Though 51 Peg A has not had enough time to synchronize its spin period with 51 Peg B's orbital period, 51 Peg B's spin period is surely tidally locked with its orbit at 4.23 days. The time for the tidal spin-down of the planet is given by

$$\tau \sim Q\left(\frac{R_p^3}{GM_p}\right)\omega_p\left(\frac{M_p}{M_*}\right)^2\left(\frac{D}{R_p}\right)^6, \quad (1)$$

where Q is the planet's tidal dissipation factor, ω_p is the planet's primordial rotation rate, M_* is the star's mass, and G is the gravitational constant. Taking $Q \sim 10^5$ and $\omega_p \sim 1.7 \times 10^{-4}$ s^{-1} (Jupiter's values), we obtain $\tau \sim 2 \times 10^6$ yr. For a giant terrestrial planet, R_p is smaller, but Q is also smaller, and so τ would not be very different. Therefore, since 51 Peg A's age is $\sim 10^{10}$ yr, 51 Peg B should always present the same face to its primary, whatever its composition.

The equilibrium effective temperature of the planet is given by the formula

$$T_{eq} \sim T_*(R_*/2D)^{1/2}[f(1-A)]^{1/4}, \quad (2)$$

and the equilibrium luminosity by

$$L_{eq} \sim L_*(1-A)(R_p/2D)^2, \quad (3)$$

where R_*, T_*, and L_* are the primary's radius, effective temperature, and luminosity, respectively, and A is the Bond albedo of the planet, which for Jupiter is ~0.35. The reflected luminosity is $L_{eq}A/(1-A)$. The factor, f, is 1 if the heat of the primary can be assumed to be evenly distributed over the planet, and 2 if only one side reradiates the absorbed heat. For 51 Peg B and an albedo of 0.35, T_{eq} is roughly 1250 K, an order of magnitude above that of Jupiter and independent of R_p and M_p. We assumed that the luminosity of 51 Peg A is 60% higher than that of our Sun (Mayor & Queloz 1995), and that absorbed heat is efficiently distributed to the night side to be radiated ($f = 1$). The latter assumption is fully justified for a gas giant or for any planet with a thick atmosphere, due to rapid zonal and meridional circulation patterns, but may be problematic for a bare "rock." If 51 Peg B were a giant terrestrial planet without an atmosphere, its temperature at the substellar point could be as high as 1500 K, above the melting point of many minerals. Needless to say, the planet's L_{eq} is unaffected by tidal locking, though the phase dependence of its brightness is.

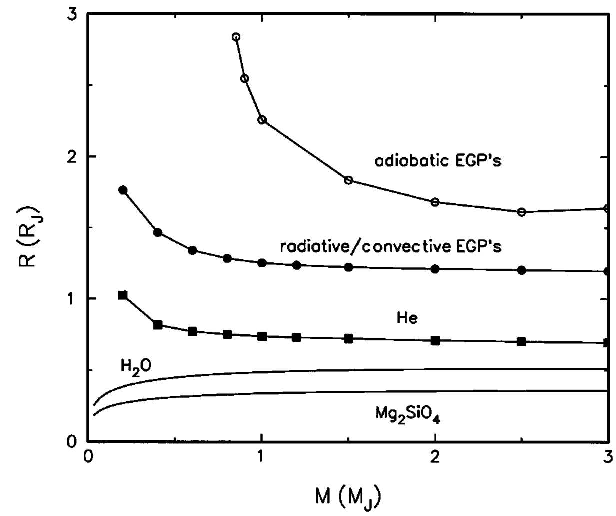

FIG. 1.—Radius (R_p) versus mass (M_p) for (*top to bottom*): fully adiabatic gas giants with surface temperature determined by radiative equilibrium with 51 Peg A; gas giants with radiative regions near the surface at the age of 51 Peg A (realistic gas-giant model); pure-helium giants with radiative/convective structure at the same age; pure H_2O models at zero temperature; pure olivine (Mg_2SiO_4) models at zero temperature. The structures of the H_2O and olivine planets were determined using the ANEOS equation of state (Thompson 1990).

Figure 1 shows the pronounced and *diagnostic* variation of radius with composition for giant planets in the mass range suggested for 51 Peg B. We have included on Figure 1 the corresponding curves for helium, H_2O, and olivine (Mg_2SiO_4) planets, as well as that for fully convective planets. The zero-temperature equations of state for H_2O and olivine (as representative of rock) were taken from the ANEOS compilation (Thompson 1990). The large mean molecular weight of giant rocky planets ensures that thermal effects are small in most of the interior (Hubbard 1984), so that an olivine or ice planet in close orbit around a star will probably not have a radius significantly larger than that predicted by our calculations. For radiative/convective gas-giant models of 51 Peg B, the predicted radii after 1 Gyr are between 1.35 and 1.9 R_J for M_ps from 2.0 to 0.5 M_J (where R_J is the radius of Jupiter). These are as much as a factor of 2 smaller than the corresponding radii for fully convective planets. After 8 Gyr (the estimated age of 51 Peg A), the radii for these same planets are between 1.2 and 1.4 R_J. Planets composed of materials with a low electron fraction per baryon and a high Z are significantly more compact (Zapolsky & Salpeter 1969). A giant terrestrial planet with a mass between 0.5 and 2.0 M_J would have a radius between 0.31 and 0.35 R_J, three times smaller than that of a gas giant in the same mass range, and its corresponding luminosity would be an order of magnitude lower ($2.0–2.5 \times 10^{-6}$ $L_\odot$). The latter depends upon the albedos assumed, but only weakly for albedos below 0.4. If photometry can be performed on 51 Peg B, a measurement of its bolometric luminosity would immediately distinguish the different models.

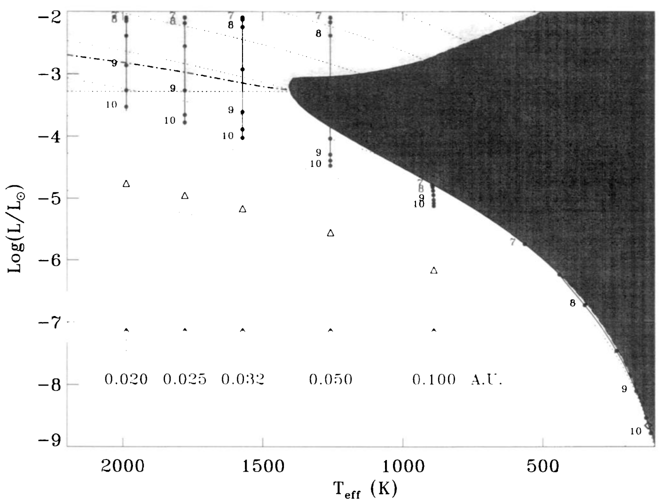

FIG. 2.—Hertzsprung-Russell diagram for 1 M_J planets orbiting at 0.02, 0.025, 0.032, 0.05, and 0.1 AU from a star with the properties of 51 Peg A, assuming a Bond albedo of 0.35. Arrows indicate the corresponding equilibrium effective temperature. A Jupiter model is also shown, the diamond in the bottom right-hand corner corresponding to the present-day effective temperature and luminosity of the planet. Evolutionary tracks for planets of solar composition are indicated by lines connecting dots which are equally spaced in log (time). The numbers 7, 8, 9, and 10 are the common logarithms of the planet's age. Zero-temperature models for 1 M_J planets made of olivine (Mg_2SiO_4) are indicated by triangles. The Hayashi forbidden region, which is enclosed by the evolutionary track of the fully convective model, is shown in dark gray (see text). Models in the light gray region have radii above the Roche limit (and therefore are tidally disrupted by the star). The region where classical Jeans escape becomes significant is bounded by the dash-dotted line. Lines of constant radius are indicated by dotted curves. These correspond, from bottom to top, to radii (in units of R_J) in multiples of 2, starting at $\frac{1}{4}$.

3. THE H-R DIAGRAM FOR GIANT PLANETS

Figure 2 is a theoretical Hertzsprung-Russell diagram that portrays the major results of this study. Depicted are L-$T_{\rm eff}$ tracks[4] for the evolution of a 1 M_J gas giant, and L for a 1 M_J olivine planet (*open triangles*; using $f = 1$), all at a variety of orbital distances (*indicated by the arrows*). Also shown are the Hayashi (1961) track (*boundary of the dark shaded region*), the Hayashi exclusion zone (*the dark shaded region itself*), the Roche exclusion zone (*the lightly shaded region*), and the classical Jeans evaporation limit (*dash-dotted line*). The shape of the Hayashi exclusion zone and the evolutionary ages depend slightly upon the atmospheric model employed. Figures such as Figure 2 can be rendered for any specific planetary mass, albedo, and primary. We focus here on $M_p = 1$ M_J, $A = 0.35$, and 51 Peg A. The dotted lines on Figure 2 are lines of constant radius. The numbers on the tracks are the common logarithms of the ages in years.

The evolution of a fully convective planet can be separated into two phases: (1) a rapid contraction phase, with large internal luminosity (converted from potential gravitational energy) and increasing effective temperature (the Hayashi boundary from the top right to the top middle of Fig. 2), and (2) a slow cooling phase during which both the internal luminosity and the effective temperature decrease (the Hayashi boundary from the top center to the bottom right of Fig. 2). The transition between these two phases occurs at R_ps around 4 R_J, regardless of the mass of the planet. The planet's internal luminosity tends to zero and its effective temperature tends to $T_{\rm eq}$. The present Jupiter is depicted by a diamond in the lower right-hand corner of Figure 2. Its evolutionary track closely follows the convective Hayashi track.

[4] Here, the luminosities do not include the reflected component.

For a given mass and composition, every fully convective model lies on the same curve in the H-R diagram. No model can exist to the right of this curve (at lower $T_{\rm eff}$). (As a corollary, any planet that lies to the left of the curve is partially radiative/conductive.) This implies that fully convective models cannot exist for large effective temperatures ($T_{\rm eff} > 1400$ K for $M_p = 1$ M_J). However, as $T_{\rm eff}$ approaches $T_{\rm eq}$, its internal luminosity drops until a radiative zone appears in the outer region and grows. This allows the luminosity and the radius of the planet to decrease further, below the values corresponding to fully convective models at the same effective temperature (i.e., the models leave the Hayashi track). At 0.05 AU, a 1 M_J planet follows the fully convective track for less than 10^7 yr. It then has a radius of about 2.5 R_J. At that point, a radiative outer region appears and the planet slowly contracts at a nearly constant effective temperature. After 8 billion years of evolution, its radius is only 1.2 R_J and its luminosity is about 3.5×10^{-5} $L_\odot$ (more than 1.5×10^4 times the present luminosity of Jupiter and only a factor of 2 below that at the edge of the main sequence). The radiative region encompasses the outer 0.03% in mass, and 3.5% in radius. The temperature is about 3100 K at 10 bar, and around 37,000 K at the center of the planet.

The quasi-static evolution of partially radiative planets is possible even for tiny star-planet separations. Such models are not unstable. At small orbital separations (below 0.04 AU), the evolution is substantially slowed down by stellar heating and the evolution tracks seen in Figure 2 are almost vertical. This is a consequence of the fact that the internal luminosity of the planet is constrained to be small. Otherwise, it would be fully convective, which is not possible at these effective temperatures. The evolutionary tracks in Figure 2 are illustrative, started for specificity at high Ls and $T_{\rm eff} = T_{\rm eq}$, inside the Roche excluded region (which is then bounded by a line of constant L, whose value is proportional to $M_p^{2/3}$). If 51 Peg B were formed beyond an AU and moved inward on a timescale greater than $\sim 10^8$ yr, it would closely follow the $R_p = R_J$ trajectory to its equilibrium position on Figure 2.

4. THERMAL AND NONTHERMAL EVAPORATION OF A GAS GIANT

If 51 Peg B is a gas giant, is it stable to evaporation and, if so, what is its current evaporation rate? We consider two potential loss mechanisms: (1) classical Jeans evaporation, and (2) the nonthermal production of hot hydrogen atoms and ions by absorption of ultraviolet radiation from 51 Peg A.

The classical Jeans escape flux is proportional to $e^{-\lambda}(\lambda + 1)$, where $\lambda = GM_p m_H / kTR_p$ (Chamberlain & Hunten 1987). Here m_H is the mass of the hydrogen atom or molecule, k is Boltzmann's constant, and T is the temperature of the planet at the escape level. For atomic hydrogen, if $T = 1300$ K, $R_p = 3$ R_J, and $M_p = 0.5$ M_J, λ is close to 30 and Jeans escape might be important. The dash-dotted line on Figure 2 is the $\lambda = 30$ line. However, this combination of parameters is unlikely for 51 Peg B (see Figs. 1 and 2). Our hydrogen-helium giant models at the age of 51 Peg A have radii closer to 1.2–1.3 R_J, and actual λs between 65 and 280. Hence, our model planets in the Mayor & Queloz mass range are much too compact for classical Jeans escape of any ion or atom to be significant.

The production and escape of hot ions (H^+ and H_2^+) and hot atomic hydrogen by stellar ultraviolet radiation is much more likely, since these fragments obtain a residual, nonthermal, kinetic energy during their production. This leaves them in the fast tail of the Jeans escape function. Using the estimate of Atreya (1986) of 3×10^9 cm^{-2} s^{-1} for the total H^+, H_2^+, and H flux from Jupiter, and assuming that the EUV flux from 51 Peg A is the same as the Sun's, we find that a gas giant at 0.05 AU with a mass of 1 M_J would lose 10^{34} Hs s^{-1}, or 10^{-16} $M_\odot$ yr^{-1}. Only ~0.5% of the mass of a 1.0 M_J gas giant at the position of 51 Peg B would be lost due to EUV radiation over the main-sequence lifetime of 51 Peg A. Since the mechanical luminosity of the solar wind is similar to the Sun's total EUV luminosity, extrapolating the Sun's wind power to 51 Peg A implies that wind ablation of 51 Peg B may be no more important. (Note that a planet composed of a higher Z material would be much less prone to evaporation or stripping.) Though these arguments suggest that a Jupiter-type planet at 0.05 AU is stable, since our derived mass-loss rates are within only 2 orders of magnitude of eroding the entire planet in its lifetime, whether evaporation affects or has affected 51 Peg B's evolution must await more rigorous calculations.

5. MODEL DIAGNOSTICS

We have shown how luminosity and radius are the primary discriminants between gas-giant and giant-terrestrial planet models for 51 Peg B. However, it may someday be possible to identify spectral signatures which can directly characterize the composition and/or origin of the object.

A primarily silicate, but Jovian-mass, planet is an unusual object which we cannot rule out. As Figures 1 and 2 demonstrate, its luminosity would be one-tenth that of a gas giant of the same mass. Its spectroscopic signature would be a strong silicate absorption band in the 10 μm wavelength region. A massive water vapor atmosphere would long ago have been photodissociated into hydrogen and oxygen, unless the abundance of water were a significant fraction (1%) of the mass of the planet.

A predominantly hydrogen-helium planet will not appear like Jupiter, even if the composition is similar. At an effective temperature of roughly 1250 K, the primary cloud-forming materials near the surface are silicates, not ammonia. However, absorption should dominate scattering, and infrared absorption features of molecular hydrogen, water, and carbon monoxide should be relatively deep and well-defined (Lunine, Hubbard, & Marley 1986). In contrast to Jupiter, methane is expected to be absent spectroscopically, because at high temperatures carbon monoxide is the thermodynamically preferred carbon-bearing molecule.

We have demonstrated in this paper that gas giants can be stable, even for very small orbital distances, and have explored the structural and thermal consequences of various models of 51 Peg B. Photometry and spectrophotometry, using very advanced interferometric and adaptive-optics techniques, may well be the key to distinguishing the different theories for the origin and nature of 51 Peg B (Angel 1994; Kulkarni 1992). However, whatever its true nature, 51 Peg B has opened a new chapter in planetary studies.

The authors would like to thank Willy Benz, Peter Hauschildt, Jim Liebert, Doug Lin, Geoff Marcy, Jay Melosh, and Andy Nelson for stimulating conversations and/or numbers in advance of publication. Gratitude is extended to the NSF and to NASA for support under grants AST93-18970 and NAG 5-2817, respectively. T. G. acknowledges support from the European Space Agency, and D. S. acknowledges NASA grant HF-1051.01-93A from the Space Telescope Science Institute, which is operated by the Association of Universities for Research in Astronomy, Inc., under NASA contract NAS5-26555.

REFERENCES

Alexander, D. R., & Ferguson, J. W. 1994, ApJ, 437, 879
Angel, J. R. P. 1994, Nature, 368, 203
Atreya, S. K. 1986, Atmospheres and Ionospheres of the Outer Planets and their Satellites (Berlin: Springer)
Boss, A. P. 1995, Science, 267, 360
Burki, G., Burnet, M., & Kuenzli, M. 1995, IAU Circ. 6251
Burrows, A., Hubbard, W. B., & Lunine, J. I. 1989 ApJ, 345, 939
Burrows, A., Hubbard, W. B., Saumon, D., & Lunine, J. I. 1993, ApJ, 406, 158
Burrows, A., Saumon, D., Guillot, T., Hubbard, W. B., & Lunine, J. I. 1995, Nature, 375, 299
Chamberlain, J. W., & Hunten, D. M. 1987, Theory of Planetary Atmospheres (2d ed.; Orlando: Academic)
Guillot, T., Chabrier, G., Gautier, D., & Morel, P. 1995, ApJ, 450, 463
Guillot, T., & Morel, P. 1995, A&AS, 109, 109
Hayashi, C. 1961, PASJ, 13, 450
Hubbard, W. B. 1984, Planetary Interiors (New York: Van Nostrand–Reinhold)
Kulkarni, S. 1992, BAAS, 24, 1220
Lin, D., Bodenheimer, P., & Richardson, D. C. 1995, Nature, submitted
Lunine, J. I., Hubbard, W. B., & Marley, M. S., 1986, ApJ, 310, 238
Marcy, G., & Butler, R. P. 1995, IAU Circ. 6251
Mayor, M., & Queloz, D. 1995, Nature, 378, 355
Noyes, R. et al. 1995, IAU Circ. 6251
Saumon, D., Bergeron, P., Lunine, J. I., Hubbard, W. B., & Burrows, A. 1994, ApJ, 424, 333
Saumon, D., Chabrier, G., & Van Horn, H. M. 1995, ApJS, 99, 713
Saumon, D., Hubbard, W. B., Burrows, A., Guillot, T., Lunine, J., & Chabrier, G. 1996, ApJ, in press
Thompson, S. L. 1990, ANEOS—Analytic Equations of State for Shock Physics Codes, Sandia Natl. Lab. Doc. SAND89-2951
Walker, G. A. H., Walker, A. R., Irwin, A. W., Larson, A. M., Yang, S. L. S., & Richardson, D. C. 1995, Icarus, 116, 359
Zapolsky, H. S., & Salpeter, E. E. 1969, ApJ, 158, 809
Zuckermann, B., Forveille, T., & Kastner, J. H. 1995, Nature, 373, 494